Multisubband electromagnetically induced transparency and coherently frozen exciton states in quantum well structures

S. M. Sadeghi*
Photonami Inc., 50 Mural Street, Richmond Hill, Ontario, Canada L4B 1E4

W. Li
Department of Chemical and Engineering Physics, University of Wisconsin-Platteville, Platteville Wisconsin 53818, USA
(Received 3 April 2005; published 19 August 2005)

We show theoretically that infrared multisubband dressing of exciton states combined with their extensive damping rates allow one to coherently make these states immune against intense resonant infrared lasers. Such coherently frozen states occur as one detects bound exciton states associated with a broad conduction subband ($e3$) when this subband is dramatically damped by emission of longitudinal optical phonons and optically coupled to a relatively narrow conduction subband ($e1$) via a two-photon coupling process. It is shown that under such conditions the exciton states are optically dressed and become stationary without any energy shift and significant amplitude change. We also use multisubband dressing of exciton states to propose a two-field electromagnetically induced transparency where enhanced quantum interference in the excitonic transitions significantly removes contributions of the bound exciton states near the band edge.

DOI: 10.1103/PhysRevB.72.075347 PACS number(s): 78.67.De, 78.66.Fd, 73.21.Fg

I. INTRODUCTION

It is well known that the interband absorption or emission in an undoped quantum well (QW) can be modified by an intense infrared (IR) laser beam polarized along the growth direction.[1,2] An example of such a process is optical quantum confined Stark effect (QCSE), in which a single IR laser is used to couple dipole transitions between the first ($e1$) and second ($e2$) conduction subbands [Fig. 1(a)].[3] This situation, which has been the source of applications for optical devices,[4,5] leads to a shift in the fundamental exciton absorption peak, causing a reduction of absorption at the frequency of the uncoupled exciton resonance.[3] Some of these investigations were also aimed at techniques to realize electromagnetically induced transparency (EIT) at the near band-edge excitonic transitions of undoped quantum wells.[6,7]

The previous studies of EIT in QWs potentially suffer from two main shortcomings. The first issue is related to the fact that in most of these studies developments of the $e1$-$hh1$ (or $e1$-$lh1$) exciton states were investigated while they were strongly coupled to the excitons associated with an upper conduction subband, i.e., the $e2$-$hh1$ (or $e2$-$lh1$) excitons using an intense midinfrared laser beam [see Fig. 1(b)].[1,6] In such a system, since the $e2$-$e1$ transition energy is more than that of longitudinal optical (LO) phonons, the $e2$-$hh1$($e2$-$lh1$) states are strongly damped by emission of such phonons. The $e1$-$hh1$ (or $e1$-$lh1$) excitons, on the other hand, are intrinsically scattered with acoustic phonons. As a result, the intrinsic damping rates of the $e1$-$hh1$ (or $e1$-$lh1$) exciton states are much smaller than those of the $e2$-$hh1$ (or $e2$-$lh1$) excitons. Such a damping configuration is not in favor of formation of EIT, as it mostly leads to a dramatic suppression of absorption peak before any coherent doubling in the exciton absorption spectrum appears.[1] This situation can even become more drastic when the excitons associated with $e1$ are localized at the potential fluctuations caused by interface roughness, impurities, and other defects. This is because the localization process can reduce the linewidths of these excitons.[8,9] The second problem comes from the fact that in order to overcome the effects caused by strong damping of the $e2$-$hh1$ (or $e2$-$lh1$) excitons and generate a transparency window in the absorption of $e1$-$hh1$ excitons in such a system [Fig. 1(b)] one needs to use an intense IR laser field resonant or near resonant with the $e1$-$e2$ transition. This, however, can lead to multilevel mixing of exciton states with different principal quantum numbers [e.g., $1s$ and $2s$ of the $e1$-$hh1$ excitons, see Fig. 1(c)].[10,11] Such a mixing process can end up with different results compared to those obtained using a simple two-level coupling system depicted in Fig. 1(b).[1,6,7]

In this paper, we show theoretically that how one can use IR-induced multisubband mixing of exciton states to (i) coherently freeze amplitude and energy of an exciton state although the quantum well structure is interacting with intense resonant IR lasers, and (ii) employ enhanced quantum interference processes to open wide transparency windows and significantly remove contributions of bound excitons near the band edge. The former occurs by establishing two-photon

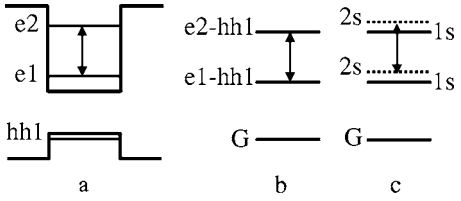

FIG. 1. (a) Schematic diagram of a square QW structure with two conduction subbands, $e1$ and $e2$. (b) represents a generic illustration of IR coupling of the excitons associated with $e1$ and $e2$, and (c) refers to the multilevel mixing of exciton states with different principal quantum numbers. The two-sided arrows refer to the mixing processes caused by the intense infrared laser beam.

dressing of the exciton states and utilizing the effects of damping rates of these states on this process. Here we use a quantum well structure where its third conduction subband ($e3$) is dramatically damped via emission of LO phonons while its first subband ($e1$) is only influenced by acoustic phonons. We show that in the presence of two intense IR lasers resonant with the $e1$-$e2$ and $e2$-$e3$ transitions the energy of the exciton associated with $e3(e3\text{-}hh3)$ remains unchanged and its amplitude is suppressed slightly. This occurs as other exciton states influenced by these fields are either dramatically suppressed or shifted.

The EIT discussed in this paper is different from those discussed before.[1,6,7] Here we use resonant multisubband optical mixing of exciton states associated $e1$, $e2$, and $e4$ with a specific configuration (see Fig. 4 inset). Such a configuration suppresses multilevel mixing of exciton states with different principal quantum numbers and reduces the field threshold required to form an EIT. The latter occurs via optical manipulation of the effective damping rate of the system that scales formation of EIT. In fact here the resonant dressing of the $e1$-$hh1$ (or $e1$-$lh1$) excitons with two sets of exciton states associated with $e2$ and $e4$ (Fig. 4 inset) forms two parallel channels of destructive quantum interference processes. Each of these channels suppresses absorption of the exciton states near the band edge, opening a wide transparency window.

Note that the EIT discussed in this paper can be used for all-optical modulators and switches at the wavelength ranges corresponding to the interband excitonic transitions. In such applications one only needs to vary the intensity one of the IR fields. This is because of the fact that if the ratio of the Rabi frequencies associated with these fields becomes far from unity, the stronger field destroys the coherence associated with the weaker field.[12] In addition, since the recovery times of such devices are determined by the dephasing rates of the conduction intersubband transitions, they are expected to be very fast. The frozen states, on the other hand, can be related to coherent population trapping of excitons. Excitons in such states are stored in a specific form of dressed state that suppresses their optical transitions into the states associated with $e2$ and vice versa.

II. MULTISUBBAND MIXING OF EXCITONS

We consider an undoped III-V semiconductor QW for which three or more bound conduction subbands are supported, in addition to several valence subbands. In the absence of any IR fields, the Hamiltonian describing the elementary excitations of this system is given by

$$H = H_0 + V. \tag{1}$$

H_0 contains the single particle energies of electrons and holes, and is given by

$$H_0 = \sum_{n_c,\mathbf{k}} E^c(n_c,k) a^\dagger_{n_c,\mathbf{k}} a_{n_c,\mathbf{k}} + \sum_{n_v,\mathbf{k}} E^v(n_v,k) a^\dagger_{n_v,\mathbf{k}} a_{n_v,\mathbf{k}}. \tag{2}$$

$E^c(n_c,\mathbf{k})$ and $E^v(n_v,\mathbf{k})$ are the electron energies for states $|n_c,\mathbf{k}\rangle$ and $|n_v,\mathbf{k}\rangle$ in the conduction and valence subbands labeled by n_c and n_v, respectively, where heavy- and light-hole valence bands are included ($v=hh,lh$), and $\mathbf{k}$ is the electron wave vector in the plane of the QW. Parabolic dispersion relations are used to describe the in-plane kinetics, where the effective masses are taken to be independent of the subband indices. $a^\dagger_{n_c,\mathbf{k}}$ and $a_{n_c,\mathbf{k}}$ are the creation and annihilation operators for electrons in the conduction subband with index n_c, and $a^\dagger_{n_v,\mathbf{k}}$ and $a_{n_v,\mathbf{k}}$ are the corresponding operators for electrons in the valence subbands. We treat the case of low interband excitation in which electron-electron and hole-hole interactions can be neglected and screening of the Coulomb interaction between the electron-hole pairs is insignificant. Coulomb mixing between different subbands is considered negligible since we focus on QW's with well width <15 nm.[13] With these considerations, the Coulomb operator in Eq. (1), which describes electron-hole interactions, is of the form

$$V = \sum_{n_c,n_v} \sum_{\mathbf{k},\mathbf{k}',\mathbf{q}\neq\mathbf{0}} V_{n_c,n_v}(\mathbf{q}) a^\dagger_{n_c,\mathbf{k}+\mathbf{q}} a^\dagger_{n_v,\mathbf{k}'-\mathbf{q}} a_{n_v,\mathbf{k}'} a_{n_c,\mathbf{k}}, \tag{3}$$

where $V_{n_c,n_v}(\mathbf{q})$ is the matrix element of the Coulomb operator between the single particle states and $\mathbf{q}$ is the wave vector exchanged in the particle interaction.

The exciton eigenstates of the total Hamiltonian in Eq. (1) may be expressed in terms of the associated free ($V_{n_c,n_v}=0$) electron ($\Psi_{n_e,\mathbf{k}}(\mathbf{r}_e)$) and hole $[\Psi_{n_h,\mathbf{k}}(\mathbf{r}_h)=\Psi_{n_v,-\mathbf{k}}(\mathbf{r}_v)]$ single particle eigenfunctions as

$$\Psi_\alpha(\mathbf{r}_e,\mathbf{r}_h) = \sum_{n_e,n_h} \sum_{\mathbf{k}} G^\alpha_{n_e,n_h}(\mathbf{k}) \Psi_{n_e,\mathbf{k}}(\mathbf{r}_e) \Psi_{n_h,\mathbf{k}}(\mathbf{r}_h), \tag{4}$$

where $G^\alpha_{n_e,n_h}(\mathbf{k})$ is the envelope function of an exciton with zero center of mass momentum, and α represents the energy index. The envelope functions may be obtained using the following equation:

$$[E^e(n_e,k) + E^h(n_h,k)] G^\alpha_{n_e,n_h}(\mathbf{k}) - \sum_{\mathbf{q}\neq\mathbf{0}} V_{n_e,n_h}(\mathbf{q}) G^\alpha_{n_e,n_h}(\mathbf{k}+\mathbf{q}) = \epsilon^{n_e,n_h}_\alpha G^\alpha_{n_e,n_h}(\mathbf{k}). \tag{5}$$

Here $\epsilon^{n_e,n_h}_\alpha$ is the transition energy of the corresponding excitons.

Let us now consider the interaction of this system with two IR fields $E(t)=Ee^{i\omega t}$ and $E'(t)=E'e^{i\omega' t}$, polarized along the QW growth direction, z. The laser frequencies ω and ω' are, respectively, taken to be resonant with the $|e1,\mathbf{k}\rangle$ to $|e2,\mathbf{k}\rangle$ ($e1$-$e2$) and the $|e2,\mathbf{k}\rangle$ to $|e3,\mathbf{k}\rangle$ ($e2$-$e3$) transitions, and are considered to be far from resonance with any other transition in the system. Note that the resonant condition for these fields is crucial, as each of these IR lasers can effectively induce multilevel mixing of exciton states with different principal quantum numbers if they are detuned from the $e1$-$e2$ or $e2$-$e3$ transitions.[11] Within the electric-dipole and rotating wave approximations, the associated interaction Hamiltonian is given by

$$H_{\text{int}} = H_1 + H_2, \tag{6}$$

where

$$H_1 = \hbar \sum_{\mathbf{k}} \{\mu_{e1e2} E(t) a^{\dagger}_{e2,\mathbf{k}} a_{e1,\mathbf{k}} + \mu^{*}_{e1e2} E^{*}(t) a^{\dagger}_{e1,\mathbf{k}} a_{e2,\mathbf{k}}\}, \quad (7)$$

$$H_2 = \hbar \sum_{\mathbf{k}} \{\mu_{e2e3} E'(t) a^{\dagger}_{e3,\mathbf{k}} a_{e2,\mathbf{k}} + \mu^{*}_{e2e3} E^{*\prime}(t) a^{\dagger}_{e2,\mathbf{k}} a_{e3,\mathbf{k}}\}. \quad (8)$$

Here μ_{e1e2} and μ_{e2e3} are the z components of the matrix elements of the electric dipole operator between single electron states in the conduction subbands.

Given the total Hamiltonian in Eq. (1) and Eq. (6), one may obtain the equations of motion for the system's density matrix,

$$\frac{\partial \rho^{\mathbf{k}}}{\partial t} = -\frac{i}{\hbar}[H + H_{\text{int}}, \rho^{\mathbf{k}}] + \left.\frac{\partial \rho^{\mathbf{k}}}{\partial t}\right|_{\text{relax}}, \quad (9)$$

to determine the effect of the IR fields on the linear interband absorption. The second term in Eq. (9) represents the corresponding damping terms in k space. Each element of the density matrix can be transferred into an excitonic basis according to

$$\rho^{\mathbf{k}}_{n_e,n_h} = \sum_{\alpha} \rho^{\alpha}_{n_e,n_h} G^{\alpha}_{n_e,n_h}(\mathbf{k}), \quad (10)$$

$$\rho^{\mathbf{k}}_{n'_e,n''_e} = \sum_{\alpha} \rho^{\alpha}_{n'_e,n''_e} G^{\alpha}_{n_e,n_h}(\mathbf{k}). \quad (11)$$

Here the sum over α includes all bound and continuum states of the chosen exciton basis associated with the n_eth and n_hth electron and hole subbands. The optical Bloch equations for this system in the exciton basis can thus be reduced to independent 16×16 matrix equations for each n_e and n_h, describing the coupling of the corresponding $n_e=e1$, $e2$, and $e3$ excitons by the IR field,

$$\frac{d\mathbf{\Phi}^{\alpha}_{n_h}}{dt} = \mathbf{L}^{\alpha}_{n_h} \mathbf{\Phi}^{\alpha}_{n_h} + \mathbf{K}^{\alpha}_{n_h}. \quad (12)$$

Here the elements of $\mathbf{\Phi}^{\alpha}_{n_h}$ are the 16 density matrix elements in the excitonic basis ($\rho^{\alpha}_{n_e,n_h}$), while $\mathbf{L}^{\alpha}_{n_h}$, a 16×16 matrix, and $\mathbf{K}^{\alpha}_{h_h}$, a 16-element column vector, contain the coefficients of the density matrix elements from the equations of motion.

To calculate the linear interband response of the IR-coupled QW to a weak optical field, we employ linear response theory.[14] From this approach, one finds that the imaginary part of the linear susceptibility $[A(\omega)]$ is expressible in terms of the two-time correlations of the system polarization, given by

$$A(\omega_t) \propto \text{Re}\left(\sum_{\alpha=1s,2s,\ldots} \langle [P^{+}_{\alpha}(t'), \tilde{P}^{-}_{\alpha}(t',z)] \rangle \big|_{z=i\omega_t} \right). \quad (13)$$

Here ω_t is the frequency of the test or probe field, and $P^{+}_{\alpha}(t)$ and $P^{-}_{\alpha}(t)$ are the positive and negative components of the contribution to the system polarization from the exciton transition specified by α. These polarization components are given by

$$P^{+}_{\alpha}(t) = \sum_{n_h,n_e} \mu^{\alpha}_{n_h,n_e} a_{n_e,\alpha} a_{n_h,\alpha}, \quad (14)$$

and $P^{-}_{\alpha}(t) = [P^{+}_{\alpha}(t)]^{*}$. $a_{n_e,\alpha}$ and $a_{n_h,\alpha}$ are the annihilation operators for an electron and hole in the αth exciton state associated with subbands with indices n_e and n_h. Due to the interband selection rules, mainly components with $n_e=n_h$ contribute to Eq. (14). This condition comes from the fact that in this paper we consider narrow square QW structures that are symmetric with respect to the center of the wells and Coulomb mixing of their exciton states is ignorable.[15,16] $\mu^{\alpha}_{n_h,n_e}$ is the dipole moment for transition from the QW ground state to an exciton state associated with n_e and n_h and energy index α. $\tilde{P}^{-}_{\alpha}(t',z)$ is the Laplace transform of $P^{-}_{\alpha}(t) = \mathrm{P}^{-}_{\alpha}(t'+\tau)$ with respect to $\tau=t-t'$, where $\tau>0$.

The two-time correlation functions in Eq. (13) are evaluated using the quantum regression theorem.[17] The density matrix elements are obtained from Eq. (12) assuming that the IR field amplitudes are slowly varying compared to the dephasing rates of the conduction subbands. In this case, we can assume that the IR fields establish a steady state with the QW, and set $d\Phi^{\alpha}_{n_h}/dt=0$. The solution to Eq. (12) in this case is given by

$$\mathbf{\Phi}^{\alpha}_{n_h}(\infty) = -[\mathbf{L}^{\alpha}_{n_h}]^{-1} \mathbf{K}^{\alpha}_{n_h}. \quad (15)$$

Using this result, the contribution to the spectral response from the αth heavy-hole exciton state is

$$\langle [P^{+}_{\alpha}(\infty), \tilde{P}^{-}_{\alpha}(z)] \rangle_{hh} = \Pi^{\alpha}_{e1\text{-}hh1} + \Pi^{\alpha}_{e2\text{-}hh2} + \Pi^{\alpha}_{e3\text{-}hh3}, \quad (16)$$

where

$$\Pi^{\alpha}_{e1\text{-}hh1} = |\mu^{\alpha}_{e1,hh1}|^2 \{R^{hh1,\alpha}_{10,5}(z) \rho^{\alpha}_{e3,hh1}(\infty) + R^{hh1,\alpha}_{10,6}(z) \rho^{\alpha}_{e2,hh1}(\infty) + R^{hh1,\alpha}_{10,7}(z) \rho^{\alpha}_{e1,hh1}(\infty) + R^{hh1,\alpha}_{10,10}(z) \rho^{\alpha}_{hh1,hh1}(\infty)\}, \quad (17)$$

$$\Pi^{\alpha}_{e2\text{-}hh2} = |\mu^{\alpha}_{e2,hh2}|^2 \{R^{hh2,\alpha}_{13,4}(z') \rho^{\alpha}_{e3,hh2}(\infty) + R^{hh2,\alpha}_{13,8}(z') \rho^{\alpha}_{e1,hh2}(\infty) + R^{hh2\alpha}_{13,13}(z') \rho^{\alpha}_{hh2,hh2}(\infty)\}, \quad (18)$$

$$\Pi^{\alpha}_{e3\text{-}hh3} = |\mu^{\alpha}_{e3,hh3}|^2 \{R^{hh3,\alpha}_{11,2}(z'') \rho^{\alpha}_{e2,hh3}(\infty) + R^{hh3,\alpha}_{11,3}(z'') \rho^{\alpha}_{e1,hh3}(\infty) + R^{hh3,\alpha}_{11,11}(z'') \rho^{\alpha}_{hh3,hh3}(\infty) + R^{hh3,\alpha}_{11,16}(z'') \rho^{\alpha}_{e3,hh3}(\infty)\}. \quad (19)$$

An analogous result applies for the light-hole excitons. The matrix $\mathbf{R}^{n_h\alpha}(z)$ is defined by

$$\mathbf{R}^{n_h\alpha}(z) = (z\mathbf{I} - \mathbf{L}^{\alpha}_{n_h})^{-1}. \quad (20)$$

$\mathbf{I}$ refers to the identity matrix, $z'=z-i\omega$, and $z''=z-i(\omega+\omega')$.

Using Eqs. (16)–(20) one may calculate the absorption spectrum of a multisubband QW structure in the presence of two IR fields with arbitrary intensities. The above theory treats the specific case in which the IR fields are resonant with the $e1$-$e2$ and $e2$-$e3$ conduction subband transitions, although similar expressions may be derived for other coupling configurations.

III. COHERENTLY FROZEN EXCITON STATES AND TWO-PHOTON DRESSING

In order to illustrate the key features of the two-field dressing process and show how it can lead to coherent freezing of exciton states, here we calculate the linear interband absorption spectrum of a $Ga_{0.47}In_{0.53}As/In_{0.52}Al_{0.48}As$ QW structure in the presence of two IR fields resonant with the $e1$-$e2$ and $e2$-$e3$ transitions. In our calculations, the QW width was taken as 10 nm. In this case, the $e1$-$e2$ and $e2$-$e3$ transition energies are 130 and 177 meV, respectively.[15] This system was studied in Ref. 18, where the low temperature (12 K) absorption spectrum was measured. We assume dephasing rates of bound states associated with $hh1$ and various electron subbands ($e1$, $e2$, and $e3$) to be $(\gamma_{e1,hh1})=2.5$ meV, $(\gamma_{e2,hh1})=5.8$ meV, and $(\gamma_{e3,hh1})=9.2$ meV, and those associated with $lh1$ are $(\gamma_{e1,lh1})=3$ meV, and $(\gamma_{e2,lh1})=6.3$ meV. The dephasing rates of excitons with a hole subband index greater than 1 are considered to be determined primarily by the electron subband index. For example, for the heavy-hole excitons we have $\gamma_{e1,hh1}=\gamma_{e1,hh2}=\gamma_{e1,hh3}$. The continuum dephasing rates were taken to be the same as those of the bound light-hole excitons. Note that the dephasing rates considered here satisfy the fact that at low temperatures the excitons associated with $e1$ are mostly scattered with acoustic phonons while those associated with $e2$ and $e3$ are influenced by the fast exciton-LO-phonon scattering processes. Therefore, the former have longer dephasing times than the latter. In addition, one expects these rates are influenced by the fact that as an upper conduction subband gets closer to the continuum, it becomes broader. Moreover, excitons in QW structures are scattered with the potential fluctuations caused by the interface roughness, alloy inhomogeneity, and other defects. These processes have significant contributions to the linewidths of the excitons discussed in this section.[18] The z component of the dipole matrix elements associated with the $e1$-$e2$ and $e2$-$e3$ transitions were assumed to be equal, with a value of $\mu_{e1e2}=\mu_{e2e3}=e\times 2$ nm. In our calculations, the Rabi frequencies of the two IR fields are taken to be equal (i.e., $\Omega_{e1e2}=\Omega_{e2e3}\equiv\Omega$). In this case, for both E and E', the relationship between the IR field intensity (I) and the Rabi frequency is $I=0.06\Omega^2$ MW/cm^{-2}, with Ω in units of ps^{-1}.

Figure 2 shows the absorption spectra of the such a structure in the absence (solid line) and presence (dashed line) of the IR fields with 24 MW/cm^2 intensity. These results indicate that these fields lead to a dramatic modification of the absorption spectrum of the QW. These modifications are primarily concentrated at frequencies in the vicinity of the bound exciton absorption lines. The nature of the IR-induced changes to the spectrum, furthermore, differs for excitons associated with different conduction subbands. For the bound excitons associated with the electrons in the first conduction subband ($e1$-$hh1$ and $e1$-$lh1$), the IR fields lead to a dramatic amplitude suppression. Although hidden to some extent, this process occurs as the spectra of these excitons each transforms into a triplet of peaks, for which the center peak occurs at the energy of the original exciton resonance. When we probe the $e3$-$hh3$ excitons, however, the situation is rather different. Although here a well-defined triplet has been developed, the amount of suppression of the central exciton peak amplitude is small. In contrast to this case, probing of the simultaneous developments of the bound excitons associated with $e2$ reveal formation of doublets, as seen from the contributions of the bound $e2$-$hh2$ and $e2$-$lh2$ excitons to the absorption spectrum in Fig. 2. These doublets occur as contributions of these excitons at their original uncoupled resonance energies have been virtually removed totally.

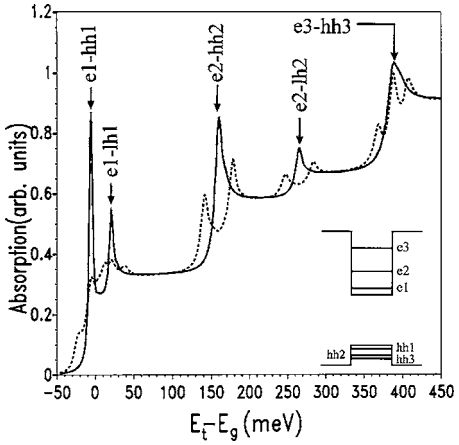

FIG. 2. Linear absorption spectra of a $Ga_{0.47}In_{0.53}As/Al_{0.48}In_{0.52}As$ QW in the absence (solid line) and presence (dashed line) of two resonant IR lasers with 24 MW/cm^2 intensity. Inset shows a schematic diagram of QW energy levels (light holes are not shown). E_t and E_g refer to the test field and band gap energies, respectively.

Two main features of the results seen in Fig. 2 are the facts that in the presence of the intense IR fields the energy of the bound $e3$-$hh3$ exciton remains unchanged and its amplitude is suppressed slightly. In order to develop an intuitive understanding for these features we have applied a dressed-state analysis to the bound exciton levels in this system, in which one- and two-photon dressing processes have been included. As discussed in Sec. II, the IR fields lead to coupling of excitons associated with electrons from different conduction subbands and holes from the same valence subband. This situation is depicted in Fig. 3(a) for the heavy-hole exciton states. (A similar set of diagrams applies to the light-hole excitons.) Here the hole subband is selected by the test or probe field energy, as only diagonal exciton states (excitons with the same electron and hole subband indices) are measurable. Figure 3(b) shows the energy levels corresponding to the stationary states of excitons involving holes from the first heavy-hole subband in the presence of the two IR fields. The eigenstates of the one- and two-photon dressed states shown in this figure are as follows:[19]

$$|t\rangle = -\frac{1}{\sqrt{2}}(|e1\text{-}hh1\rangle_\alpha - |e3\text{-}hh1\rangle_\alpha), \tag{21}$$

$$|s\rangle = \frac{1}{\sqrt{2}}\left(\frac{1}{\sqrt{2}}|e1\text{-}hh1\rangle_\alpha + |e2\text{-}hh1\rangle_\alpha + \frac{1}{\sqrt{2}}|e3\text{-}hh1\rangle_\alpha\right), \tag{22}$$

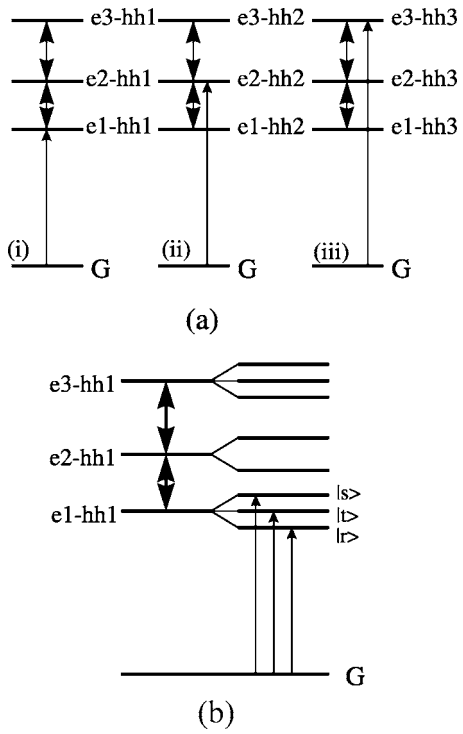

FIG. 3. (a) Schematic diagram of IR coupling processes when the probe field is tuned to the (i) $e1$-$hh1$, (ii) $e2$-$hh2$, or (iii) $e3$-$hh3$ exciton resonances. The thick two-sided arrows refer to coupling of exciton states by the intense IR laser fields, and the thin one-sided arrows refer to transitions induced by a weak interband test field. (b) Schematic diagram of the dressed-state picture for the coupling processes in (i). The dressed state $|t\rangle$ arises from a dominant two-photon coupling process, while $|s\rangle$ and $|r\rangle$ originate from one-photon coupling.

$$|r\rangle = \frac{1}{\sqrt{2}}\left(\frac{1}{\sqrt{2}}|e1\text{-}hh1\rangle_\alpha - |e2\text{-}hh1\rangle_\alpha + \frac{1}{\sqrt{2}}|e3\text{-}hh1\rangle_\alpha\right). \tag{23}$$

These equations show how the dressing of exciton states under one- ($|s\rangle$ and $|r\rangle$) and two-photon ($|t\rangle$) dressing occur. As indicated in Fig. 3(b), similar set of equations also holds when we detect the exciton states associated with $e3$.

Investigation of the eigenstates of Eqs. (21)–(23) explains why the central peaks remain at the uncoupled exciton energies, irrespective of the magnitudes of the resonant IR laser intensities. To see this note that in a dressed-state picture $|t\rangle$, $|r\rangle$, and $|s\rangle$ are the eigenfunctions of H_{int} [Eq. (6)],

$$H_{\text{int}}|t\rangle = 0, \tag{24}$$

$$H_1|s\rangle = \hbar\sqrt{2}\Omega|s\rangle, \tag{25}$$

$$H_1|r\rangle = -\hbar\sqrt{2}\Omega|t\rangle. \tag{26}$$

As one can see here the eigenvalues of the two-photon states are zero, indicating no shift due to the resonant infrared lasers. This feature only partially explains how one can freeze an exciton state. Another issue is related to the amplitudes of the two-photon states. In fact our investigation has shown that when one detects $e1$-$hh1$ excitons the ratio of amplitude of the bound exciton states in the absence of the IR fields (A_0) to that of the central peak in the presence of these fields (A_c) are given by

$$\left.\frac{A_0}{A_c}\right|_{e1} = \frac{\gamma_{e1,hh1} + \gamma_{e3,hh1}}{\gamma_{e1,hh1}}. \tag{27}$$

However, when one detects the $e3$-$hh3$ exciton states this ratio becomes

$$\left.\frac{A_0}{A_c}\right|_{e3} = \frac{\gamma_{e3,hh3} + \gamma_{e1,hh3}}{\gamma_{e3,hh3}}. \tag{28}$$

The width of the central two-photon state is also given by

$$W_c = \gamma_{e1,hh3} + \gamma_{e3,hh3}, \tag{29}$$

irrespective of the which exciton is detected. Equations (27)–(29) show the conditions where an exciton state can be coherently transformed into a frozen state with nearly the same amplitude as that of the uncoupled exciton at the same energy. Based on Eq. (27), since $\gamma_{e1,hh1} < \gamma_{e3,hh1}$ one expects a dramatic suppression of absorption amplitude when $e1$-$hh1$ is detected, as seen in Fig. 2. Such a condition, however, works in favor of small amplitude change when $e3$-$hh3$ is detected, as can be seen in Eq. (28). Note that as shown in Eq. (29), this process comes at the cost of narrowing the linewidth of the bound $e3$-$hh3$ absorption spectrum. The effect of such a narrowing process can be seen in Fig. 2 around the $e3$-$hh3$ exciton energy. Note that the effects discussed in this paper become more distinct and resolved if $e1$-$hh1$ excitons become localized.

Note that the frozen exciton states discussed above are related to coherent population trapping (CPT) of excitons. This phenomenon, which has already been discussed in atomic systems[20] and quantum wells,[21] happens in general when two bound states are coupled to an upper broad state or the continuum by two laser fields. The efficient two-photon coupling between the bound states traps electrons in a state that is an antisymmetric superposition of the bound states, similar to $|t\rangle$ in Eq. (21). Under these conditions due to destructive quantum interference, optical excitation of electrons from the bound states into the broad state or continuum is suppressed. In the system discussed in this section formation of the frozen state is an indication of coherent trapping of part of exciton population in the $|t\rangle$ associated with $e3$. The optical transitions from this state to those associated with $e2$ or vice versa are therefore suppressed. Under this condition some of the excitons are also trapped in the $|t\rangle$ associated with the central peak of the $e1$-$hh1$ or $e1$-$lh1$ states near the band edge.

IV. MULTISUBBAND ELECTROMAGNETICALLY INDUCED TRANSPARENCY OF NEAR BAND-EDGE EXCITONS

The possibility of fabricating an all-optical absorption switch based on coherent intersubband mixing in undoped QW's is very attractive since such a device would be extremely fast, the recovery time being limited only by the

coherence decay time between the conduction subbands. An optimal design for such a device would incorporate the largest IR-induced changes in absorption with the lowest IR field intensities possible. In this section, we use multisubband mixing of excitons to present a scheme which can lead to an enhanced EIT. In such a scheme the bound state exciton absorption may be removed significantly. As mentioned in the introduction, this result is in contrast to the optical schemes employing the conventional optical QCSE or EIT (Fig. 1),[1,6] where multilevel mixing of exciton states with different principal quantum numbers and/or strong damping of $e2$-$hh1$ (or $e2$-$lh1$) can hinder an effective coherent reduction of absorption near the band edge.

The physical signatures of the enhanced EIT have already been depicted in Fig. 2. The well-resolved doublet seen near the continuum edge of the $e2$-$hh2$ excitons is a peculiar EIT associated with the $1s$ bound states of these excitons. Such a EIT was, however, embedded on the continua of the $e1$-$hh1$ and $e1$-$lh1$ excitons. A more useful case is generation of such a phenomenon near the band edge of a QW. To study this case in this section we consider a $Ga_{0.47}In_{0.53}As/InP$ QW with 14 nm well width in the presence of two IR fields. This structure contains three bound conduction subbands ($e1$, $e2$, and $e3$) and one quasibound subband ($e4$) in the continuum of the conduction band. We consider the first field is tuned in resonance with the transition between the first and fourth conduction subbands, and so couples excitons associated with $e1$ and $e4$. The second field is resonant with the $e1$-$e2$ transitions (see inset of Fig. 3). For our calculations, we considered $\gamma_{e1,hh1}=1.5$, $\gamma_{e2,hh1}=3.1$, and $\gamma_{e4,hh1}=13.2$ meV, and for the light holes, dephasing rates of $\gamma_{e1,lh1}=2$, $\gamma_{e2,lh1}=3.6$, and $\gamma_{e4,lh1}=14.5$ meV were used. As in the preceding section, the dephasing rates of excitons with a hole subband index greater than 1 are considered to be determined primarily by the electron subband index. The dephasing rates of the exciton continuua were considered to be the same as those of the bound light-hole excitons. These rates were chosen to reflect typical sample conditions, including interface roughness. For the calculations presented in this section, the field strengths are chosen such that $\Omega_{12}=\Omega_{14}\equiv\Omega$. Since we are interested in absorption modifications in the vicinity of the band edge, we focus on the effect of the IR fields on the $e1$-$hh1$ and $e1$-$lh1$ exciton states.

The calculated absorption spectra of the IR-coupled QW is shown in Fig. 4 for three different values of Ω. The solid line indicates the absorption profile in the absence of IR coupling, while the dashed and dotted lines show the modified spectrum for $\Omega=25$ and 50 ps^{-1}, respectively. The absorption spectrum of the uncoupled QW exhibits two large peaks corresponding to the heavy-hole and light-hole exciton resonances. In the presence of the IR fields, each of these original peaks is replaced by a pair of lines occurring on either side of the original resonance energy. The energy separation between these two lines increases with increasing field intensities.

As in the case of the $e2$-$hh2$ and $e2$-$lh2$ excitons investigated in the preceding section, since in the case of Fig. 4 there is no resonant two-photon dressing of the exciton states, no peak at the uncoupled exciton resonance can be generated. Here the satellite peaks correspond to the formation of the pairs of one-photon IR dressed levels. Therefore, as illustrated in Fig. 4, a strong reduction in oscillator strength occurs at the frequencies of the uncoupled exciton resonances. The threshold intensity for generation of such a multisubband EIT is scaled by

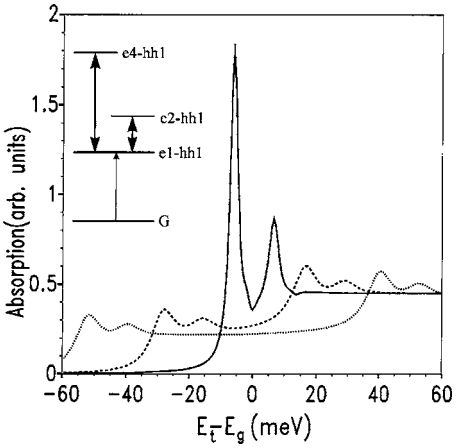

FIG. 4. Absorption spectra of a $Ga_{0.47}In_{0.53}As/InP$ quantum with 14 nm well width interacting with two intense IR laser beams (inset). Solid, dashed, and dotted lines refer, respectively, to spectra in the absence and presence of the infrared lasers with $\Omega=25$ and 50 ps^{-1}. E_t and E_g refer to the test field and band gap energies, respectively.

$$\gamma_{\text{eff}}=\frac{\gamma_{e4,hh1}\gamma_{e2,hh1}}{\gamma_{e4,hh1}+\gamma_{e2,hh1}}. \tag{30}$$

This finding indicates that lower IR field strengths are required to achieve effective absorption switching in our system than in one which applies a single IR field to couple exciton states associated with $e1$ and $e2$ or with $e1$ and $e4$. This is because the lower limit on the switching intensity is determined by an effective dephasing rate (γ_{eff}) which is lower than the rates associated with single field coupling ($\gamma_{e2,hh1}$ or $\gamma_{e4,hh1}$). This feature becomes more distinctively clear if one compares the case where two IR fields are used with the case in which only a single IR field resonant with the $e1$-$e4$ transition interacts with the QW structure. We found that for the latter when $\Omega=25$ ps^{-1} the reduction of absorption at the uncoupled exciton resonance was at least 15% less than the corresponding case in Fig. 4. Such a difference becomes more dramatic at lower field intensities. This is because of the fact that at such intensities the evolution of absorption spectrum is much more sensitive to the IR field intensities.

The enhanced EIT discussed here corresponds to IR-induced redistribution of the exciton oscillator strength, causing nearly full removal of the bound state absorption at the uncoupled exciton frequency. The residue of absorption mostly comes from the hh and lh exciton continua. Such a EIT can be associated with an enhanced form of quantum interference in the excitonic transitions of the QW structure. As shown in Fig. 5, here the interfering paths consist of one direct (i) and two Raman paths (ii) and (iii). The direct path (i) occurs between the QW ground state to $e1$-$hh1$, and the

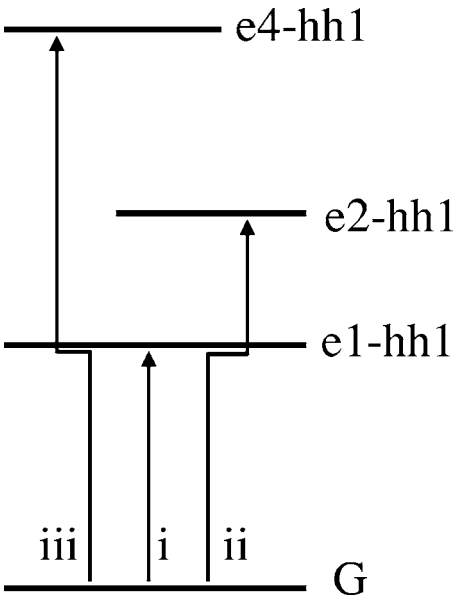

FIG. 5. Schematic diagram of the interfering paths involved in the multisubband LIT shown in Fig. 4.

Raman paths are indirect transitions between the QW ground state to $e2$-$hh1$ (ii) and $e4$-$hh1$ (iii). Here since the Raman paths are not correlated, they cause two dissociated interference processes between (i) and (ii) and between (i) and (iii). The result is generation of two transparency windows overlapping with each other at the uncoupled resonance of $e1$ -$hh1$. This is in fact the key mechanism behind the enhanced LIT caused by two IR fields. The high extinction ratio here can also be related to the fact that, instead of 2Ω as in the case of single field coupling, the doublet peaks in the case of two-infrared coupling are separated from each other by $2\sqrt{2}\Omega$.

V. CONCLUSIONS

In conclusion, we have theoretically demonstrated the effects of multisubband optical dressing of exciton states in the interband absorption spectra of quantum well structures. We showed that when such a dressing is caused by two intense infrared lasers resonant with the $e1$-$e2$ and $e2$-$e3$ transitions, the energy of the $e3$-$hh3$ exciton remained unchanged and its amplitude became relatively immune against the field intensities. We associated these results with the two-photon dressing of the excitons associated with $e1$ and $e3$ and the effects of the strong damping of $e3$-$hh3$ caused by LO-phonon emission. Our calculations also showed that multisubband dressing of exciton states could lead to an enhanced form of EIT in which an IR-induced redistribution of oscillator strength leads to a significant removal of the bound state absorption at the fundamental exciton resonances. We associated these effects with an enhanced form of quantum interference in the QW excitonic transitions.

*Present address: Department of Electrical and Computer Engineering, McMaster University, Hamilton, Ontario, Canada L8S 4K1. Electronic address: sm.sadeghi@utoronto.ca

[1] D. Frohlich, C. Neumann, S. Spitzer, and R. Zimmermann, in *Optics of Excitons in Confined Systems, Giardini Naxos*, edited by A. D. Andrea, R. D. Sole, R. Girlanda, and A. Quatropani (IOP, Bristol, 1991), Vol. 123, p. 227.
[2] S. M. Sadeghi and J. Meyer, J. Phys.: Condens. Matter **12**, 5801 (2000).
[3] D. Frohlich, R. Wille, W. Schlapp, and G. Weimann, Phys. Rev. Lett. **59**, 1748 (1987).
[4] A. Neogi, H. Yoshida, T. Mozume, and O. Wada, Opt. Commun. **159**, 225 (1999).
[5] A. Neogi, Y. Takahashi, and H. Kawaguchi, IEEE J. Quantum Electron. **33**, 2060 (1997).
[6] A. Liu and C.-Z. Ning, J. Opt. Soc. Am. B **17**, 433 (2000).
[7] D. S. Lee and K. L. Malloy, IEEE J. Quantum Electron. **30**, 85 (1994).
[8] J. Hegarty, M. D. Sturge, C. Weisbuch, A. C. Gossard, and W. Wiegmann, Phys. Rev. Lett. **49**, 930 (1982).
[9] H. Hillmer, A. Forchel, R. Sauer, and C. W. Tu, Phys. Rev. B **42**, 3220 (1990).
[10] S. M. Sadeghi, J. Meyer, T. Tiedje, and M. Beaudoin, IEEE J. Quantum Electron. **36**, 1267 (2000).
[11] S. M. Sadeghi and W. Li, Phys. Rev. B **69**, 045311 (2004).
[12] S. M. Sadeghi and J. Meyer, Phys. Rev. B **53**, 10094 (1996).
[13] B. Zhu and K. Huang, Phys. Rev. B **36**, 8102 (1987).
[14] R. Kubo, J. Phys. Soc. Jpn. **12**, 570 (1957).
[15] G. Bastard, *Wave Mechanics Applied to Semiconductors Heterostructures* (Les Editions de Physique, Les Ulis, France, 1998).
[16] B. Zhu, Phys. Rev. B **37**, 4689 (1988).
[17] M. Lax, Phys. Rev. **172**, 350 (1968).
[18] G. Livescu, D. A. B. Miller, D. S. Chemla, M. Ramaswamy, T. Y. Chang, N. Sauer, A. C. Gossard, and J. H. English, IEEE J. Quantum Electron. **24**, 1677 (1988).
[19] S. M. Sadeghi, J. F. Young, and J. Meyer, Phys. Rev. B **56**, R15557 (1997).
[20] E. Arimondo, in *Progress in Optics*, edited by E. Wolf (Elsevier Science, Amsterdam, 1996), Vol. XXXV, p. 257.
[21] S. M. Sadeghi and H. M. van Driel, Phys. Rev. B **63**, 045316 (2001).